Available online at www.sciencedirect.com
SCIENCE DIRECT
Journal of Catalysis 226 (2004) 466–470
JOURNAL OF CATALYSIS
www.elsevier.com/locate/jcat

Research Note

On the role of aluminum in the selective oxidation of benzene to phenol by nitrous oxide over iron-containing MFI zeolites: an in situ Fe XANES study

Emiel Hensen [a,*], Qingjun Zhu [a,1], Pang-Hung Liu [b], Kuei-Jung Chao [b], Rutger van Santen [a]

[a] *Schuit Institute of Catalysis, Eindhoven University of Technology, P.O. Box 513, 5600 MB Eindhoven, The Netherlands*
[b] *Department of Chemistry, National Tsing Hua University, Kuang Fu Road, Hsinchu 30043, Taiwan, Republic of China*

Received 5 April 2004; revised 4 June 2004; accepted 8 June 2004

Available online 20 July 2004

Abstract

In situ Fe *K*-edge XANES experiments point to a distinct difference in reducibility of iron in Fe-silicalite (without aluminum) and FeZSM-5 (with aluminum) upon dehydration. Whereas a noticeable part of Fe^{3+} is reduced to ferrous ions in the iron-containing aluminosilicalite, the ferric species in the ferrosilicalite maintain their oxidation state. The ability to selectively oxidize benzene to phenol with nitrous oxide in ferroaluminosilicalite relates to these Fe^{2+} centers. It is proposed that the large difference in reactivity between ferroaluminosilicalite and ferrosilicalite is due to the chemical difference of iron in Fe–O–Al and Fe–O–Fe adducts. A new preparation method is introduced which leads to more selective and stable catalysts.

Keywords: ZSM-5; Iron; Nitrous oxide; Phenol; Benzene; X-ray absorption spectroscopy; Oxidation state

1. Introduction

The molecular-sized dimensions of the intracrystalline pores in zeolites endow these materials with the unique property to stabilize nanometer-sized metal oxide clusters which cannot form over more open surfaces. These particles often exhibit unusual catalytic properties [1]. Intrazeolite iron-oxo complexes have attracted wide-spread attention in the field of environmental catalysis. Among other things, these zeolites can decompose nitrous oxide at low temperature, giving molecular nitrogen and an adsorbed oxygen atom. This oxygen atom can desorb as molecular oxygen with another oxygen atom or can be selectively inserted into the C–H bond of aromatics [2]. Although there has been considerable divergence of opinion as to the nature of the active sites (Brønsted acid sites [3], extraframework (EF) Al Lewis acid species [4–6] and EF Fe species [2]), evidence is piling up that the active sites contain Fe [7,8]. On the other hand, the role of aluminum, if at all, is not clear yet. Besides the assignment of Al as active sites in the form of Brønsted [3] or Lewis [4–6] acid sites, it has also been put forward that Al facilitates the removal of Fe from framework positions [9] and may provide the negative framework charge to accommodate cationic Fe complexes [2,7,10].

^{57}Fe Mössbauer spectroscopic data [7] show that nitrous oxide decomposition goes with the oxidation of Fe^{2+} to Fe^{3+} states. Ferrous species are formed upon (hydrothermal) treatment of iron-containing zeolites at high temperatures [7,11]. The active sites have been proposed to consist of cationic binuclear hydroxide- or μ-oxo-bridged Fe complexes [1,7,12,13] compensating the negative zeolite framework charge. However, our recent work [8,14,15] provides indications that also intracrystalline neutral iron–aluminum-oxide (Fe–O–Al) species should be considered as the active sites. Ferrosilicalite with trace levels of Al has a negligible

* Corresponding author. Fax: +31-40-2455054.
E-mail address: e.j.m.hensen@tue.nl (E. Hensen).
[1] Current address: Tokyo Institute of Technology, Chemical Resources Laboratory, 4259 Nagatsuta, Midori-ku, Yokohama, Japan.

0021-9517/$ – see front matter
doi:10.1016/j.jcat.2004.06.010

activity but can be activated by dispersing Al in the micropores [8]. This suggests that aluminum plays an important role in the catalytic cycle or in the formation of the active Fe^{2+} sites.

In the present contribution, we employ X-ray absorption near-edge spectroscopy (XANES) at the Fe *K* edge to follow the oxidation state and coordination of iron in steam-activated ferrosilicalite and ferroaluminosilicalite. In principle, analysis of the features well above the *K* edge (EXAFS) provides information on the type of coordinating atoms and first-shell iron-ligand distances, but this has proven to be difficult for very dispersed Fe species in zeolites [16]. However, the edge region and in particular the features in the region of the 1s → 3d transition give insight into the oxidation state and geometry of the iron atoms [16–25].

2. Experimental

Iron- and aluminum-substituted silicates of the MFI topology were synthesized by controlled hydrolysis of tetraethylorthosilicate in the presence of tetrapropylammonium hydroxide (TPAOH). To this end, TEOS (Acros, 98%) was added to TPAOH (Fluka, 20% in water) and mixed well overnight. An appropriate amount of this solution was subsequently dropwise added to solutions of iron nitrate ($Fe(NO_3)_3{\cdot}9H_2O$, Merck, 98%), aluminum nitrate ($Al(NO_3)_3{\cdot}9H_2O$, Janssen, 99%) or a mixture of iron and aluminum nitrate under vigorous stirring. The final TPAOH/Si and H_2O/Si ratios were 0.3 and 35, respectively. The mixture was transferred into a PEEK-lined autoclave and kept at 443 K for 5 days. After filtration, washing and drying at 383 K overnight, the organic template was carefully removed by treatment in a N_2 flow (100 ml min^{-1}) whilst heating to 823 K at a ramp rate of 1 K min^{-1}, followed by an isothermal period of 8 h. The sample was further treated in a O_2/N_2 flow (20 vol% O_2, 100 ml min^{-1}) at 823 K for another 4 h. Subsequently, the materials were steamed by contacting them with a water-containing artificial air flow (10 ml H_2O min^{-1}, 18 ml O_2 min^{-1}, 72 ml N_2 min^{-1}) at 973 K for 3 h. These samples are denoted by [X]MFI, where X represents the hetero-atom(s) being Fe or Al or a combination thereof. Another set of samples was prepared by pore-volume impregnation of silicalite-1 with appropriate solutions of iron nitrate or a combination of iron and aluminum nitrate. The silicalite-1 sample was hydrothermally prepared according to the same procedure as described above without addition of iron or aluminum. After impregnation, the catalysts were carefully dried and either calcined or steamed. These samples are referred to as silicalite-1-Imp(X) where X stands for Fe or Fe,Al.

Fe *K*-edge XAS measurements were performed at beamline 17C of the National Synchrotron Radiation Research Center in Hsinchu (Taiwan). The electron energy and ring current were 1.5 GeV and 160 mA, respectively. A Si(111) monochromator with an energy resolution of ∼ 0.5 eV at the Fe *K* edge was used. The main limitation for the energy resolution is the finite core-hole width, that is, ∼ 1.15 eV at the Fe *K* edge. In this case, the data were taken at an energy interval of 0.5 eV. Subsequently, they were splined by a cubic-spline method to enable curve fitting. Zeolite samples were pressed into self-supporting wafers and placed in a controlled atmosphere cell. Spectra in the XANES region (spectral range 7090–7150 eV) were recorded in fluorescence mode during a temperature-programmed heating treatment in flowing He (room temperature → 353 K at 5 K min^{-1}, 353 K → 433 K at 1.5 K min^{-1}, 433 K → 723 K at 5 K min^{-1}). After each experiment an iron reference foil was used to provide accurate energy calibration. All spectra were normalized according to standard procedures. In order to extract the pre-edge feature, the contribution of the edge jump to this feature was modeled using a cubic-spline function. The spectra were fitted with pseudo-Voigt functions.

Reaction data were collected in a single-pass atmospheric plug-flow reactor. Typically, 100 mg of catalyst was diluted with an amount of SiC to obtain a catalyst bed of 2 cm in height. Gas-phase analysis was performed by a well-calibrated combination of GC and MS. Prior to reaction, the catalyst was pre-treated in a flow of 100 ml min^{-1} O_2/He (20 vol% O_2) whilst heating to 823 K at a rate of 2 K min^{-1}. Benzene oxidation was carried out by feeding a mixture of C_6H_6/N_2O/He (volume ratio = 1:4:95) at a flow rate of 100 ml min^{-1} at a reaction temperature of 623 K.

3. Results and discussion

Relevant (reaction) data on the catalytic materials are collected in Table 1. In short, [Fe]MFI shows an almost negligible phenol productivity in line with our earlier report [8]. [Fe,Al]MFI, on the other hand, exhibits an initial phenol productivity of 6.8 mmol g^{-1} h^{-1}. Fig. 1 compares the XANES spectra for these two zeolites recorded during heating in helium. Qualitatively, one clearly observes the strong change in the edge position of [Fe,Al]MFI as compared to that

Table 1
Elemental compositions of zeolites and the phenol productivities after calcination or steaming activation pretreatments

Sample	wt% Fe	wt% Al	Treatment	R_{phenol}[a]
[Fe]MFI	0.55	< 0.005	Steaming	< 0.2
[Fe,Al]MFI	0.51	0.94	Steaming	6.8
[Fe]MFI + Me_3Al	0.55	1.4	Calcination	1.9
	0.55	1.4	Steaming	4.9[b]
Silicalite-1	< 0.001	< 0.005	Calcination	0.0
	< 0.001	< 0.005	Steaming	0.0
Silicalite-1-Imp(Fe)	0.62	< 0.005	Steaming	< 0.05
Silicalite-1-Imp(Fe,Al)	0.61	0.98	Calcination	0.3
	0.61	0.98	Steaming	4.9

[a] Phenol productivity in mmol g^{-1} h^{-1} after 5 min (reaction conditions: $T = 623$ K, feed: 1% C_6H_6, 4% N_2O, GHSV = 30,000 h^{-1}).
[b] Ref. [8].

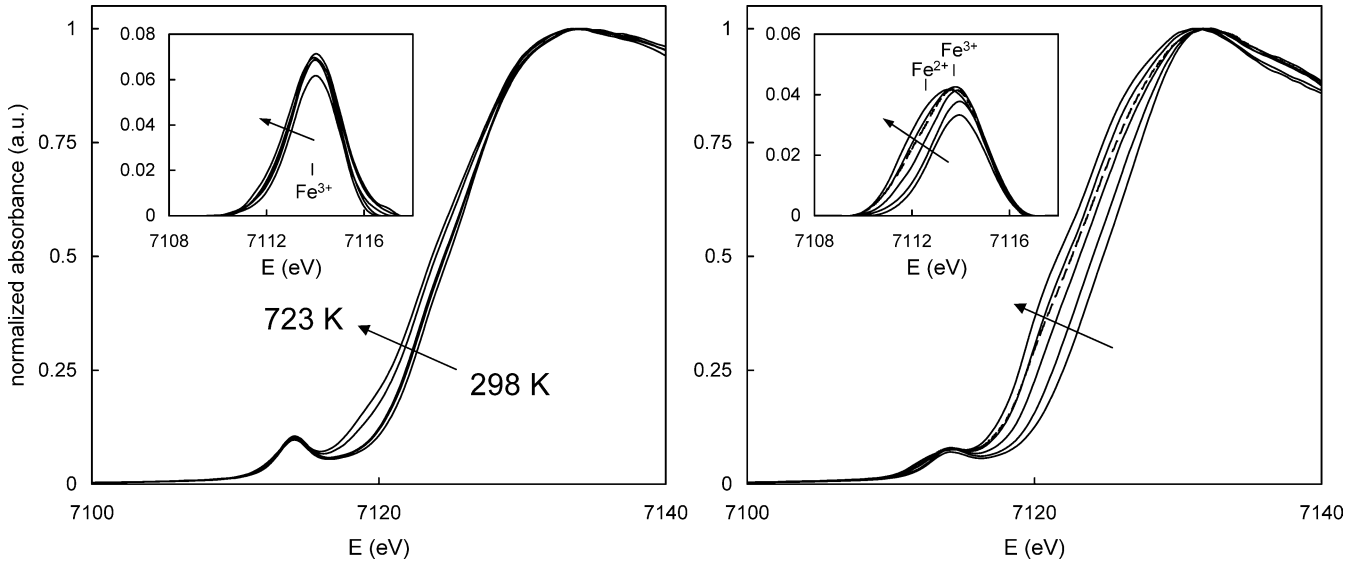

Fig. 1. Evolution of XANES spectra of steam-activated [Fe]MFI (left) and [Fe,Al]MFI (right) as a function of the dehydration temperature. The spectra were recorded at 298 K (wet), 373 K, 473 K, 573 K and 723 K. The arrow indicates the temperature increase. The insets show the corresponding pre-edge features (1s → 3d transition) after background subtraction. The XANES spectrum of [Fe,Al]MFI after cooling to room temperature is indicated by the dashed line.

Table 2
Pre-edge characteristics of steam-activated [Fe]MFI and [Fe,Al]MFI at various stages during dehydration

Sample	Edge energy (eV)	Ferric state I (Centroid)[a]	Ferrous state I (Centroid)[a]
[Fe]MFI			
RT, wet	7123.5	0.14 (7113.7)	–
723 K	7123.0	0.13 (7113.7)	0.006 (7112.3)
RT, dry	7123.2	0.15 (7113.7)	–
[Fe,Al]MFI			
RT, wet	7124.2	0.079 (7113.7)	0.005 (7112.2)
723 K	7120.0	0.070 (7113.7)	0.072 (7112.4)
RT, dry	7120.4	0.080 (7113.7)	0.053 (7112.4)

[a] Intensities (I) ± 10%; centroid position (eV) ± 0.5 eV.

of [Fe]MFI. The corresponding fit parameters for the pre-edge position are collected in Table 2. The XANES spectra of [Fe]MFI remain largely unaltered up to temperatures of 473 K with an edge energy characteristic for Fe^{3+}. This is consistent with the invariance of the pre-edge peak position. The pre-edge centroid is at 7113.7 eV which is close to the value reported for ferric compounds [16–25]. The total intensity (0.14) corresponds to the value for hematite [17] while the small increase in the intensity with temperature stems from changes in the coordination and/or geometry around iron [18], most likely due to removal of coordinating water molecules [23]. At temperatures above 473 K we observe a small shift of the edge energy to lower values (7123.5 → 7123.0 eV) together with the appearance of a very weak shoulder in the pre-edge feature with a centroid position of 7112.3 eV. This could imply the presence of a very small amount of ferrous ions. The separation between the two pre-edge centroid positions corresponds to the typical separations of the order of 1.4 eV that have been reported for ferrous and ferric ions [17,18]. After cooling the minor Fe^{2+} component disappeared again. On the contrary, dehydration of steam-activated [Fe,Al]MFI results in extensive iron reduction as evidenced by the large shift in the edge energy (7124.2 → 7120.0 eV). The decrease is strongest in the temperature range of 473–573 K. The pre-edge of the wet precursor is dominated by the contribution of ferric ions but it already contains a small amount of ferrous ions. The large difference in total intensity of the ferric component between [Fe,Al]MFI and [Fe]MFI points to a different coordination and/or geometry of a considerable part of iron. In a centrosymmetric environment (e.g., octahedral symmetry), the 1s → 3d transition is electric dipole forbidden and intensity can only be gained by weak electric quadrupole coupling [18]. The loss of the inversion center in tetrahedral coordination results in a more intense pre-edge feature [17,18]. Although the strong pre-edge for [Fe]MFI may in principle result from framework location of Fe^{3+} atoms [16], UV–vis spectra (not shown) suggest that almost all lattice Fe^{3+} species have migrated to EF positions during steaming. The supposition that at least part of Fe is not present in the framework coheres with the finding that [Fe]MFI can be activated by addition of Al and subsequent calcination (see Ref. [8] and Table 1). An alternative proposal is that a considerable portion of the Fe ions in [Fe,Al]MFI is present in a different, more symmetrical iron coordination. This could relate to the presence of cationic mononuclear [26] or binuclear [1,7] iron complexes but also to neutral EF Fe–O–Al species [8]. The presence of a small amount of Fe^{2+} in the wet [Fe,Al]MFI precursor is in line with earlier Mössbauer results [7]. A temperature increase leads to a strong increase of the contribution of this component, while that of Fe^{3+} ions decreased only slightly. This could suggest that the symmetry is lowered during reduction which can be due to the removal of oxygen [23]. It could also imply that part

of Fe is present as hematite and cannot be reduced, while another part reduces from octahedral ferric to less symmetric ferrous states. Such an interpretation agrees with the notion of a relatively low amount of active sites in these materials [7,14]. It is worthy of note that it seems that a small portion of the Fe^{2+} ions in [Fe,Al]MFI has reoxidized after cooling to room temperature.

Thus, there is a distinct difference in the reducibility of Fe^{3+} in steam-activated [Fe]MFI and [Fe,Al]MFI zeolites. An almost negligible part of iron in the former undergoes self-reduction. In the aluminum-containing zeolite, a considerable portion of Fe^{3+} ions is reduced to Fe^{2+} upon heating in helium. This difference implies the involvement of Al in the formation of Fe^{2+} centers. At the moment, we cannot conclude whether these are framework or extraframework Al sites. Hence, these results support the notion that aluminum is a required component to form those iron species that display the unusual redox properties [7,8,14,27]. One may tacitly assume that the small Fe^{2+} contribution in [Fe]MFI derives from the minor Al content in [Fe]MFI and explains the very low, but non-negligible phenol productivity (Table 1). The self-reduction of iron-containing MFI zeolites has been described earlier by several groups [19–25]. In the case of overexchanged Fe/ZSM-5 materials Fe^{2+} has been identified upon thermal activation [21–26]. Obviously, these materials contain a significant amount of aluminum. In contrast to the present study, the extensive studies of Berlier et al. [19,20] have shown that a portion of the ferric ions can undergo self-reduction in Fe-silicalite upon evacuation at 773 K. The ferrous ions could reoxidized by exposure to nitrous oxide. These results are at variance with the present ones. Relevant differences are the somewhat higher activation temperature and the vacuum treatment of Berlier et al. Although not conclusive, we suggest that the small amount of ferrous ions in the Fe-silicalite sample of Berlier et al. could be due to the presence of a small amount of aluminum, which inevitably arises in preparation routes employing sodium silicate [20]. In this respect, we stress that it is extremely important to compare Fe-silicalite and HZSM-5 materials that contain only minute small amounts of Al and Fe, respectively, with FeZSM-5 ones [8].

Based on our earlier reports [8,14,15] that have suggested the possibility of an extraframework Fe–O–Al adduct as the active species and the present results that underline the importance of the presence of Al, we prepared two additional catalysts from an inactive silicalite-1 sample and impregnated this with (i) a solution of iron nitrate or (ii) a solution of iron and aluminum nitrate. The phenol productivities of these zeolites are summarized in Table 1 and displayed in Fig. 2. Clearly, silicalite-1 to which only iron has been added is inactive, whereas a zeolite that additionally contains aluminum shows a good phenol productivity. This provides further support for the important role of aluminum. We also included the much lower value for phenol productivity of the calcined material. The positive effect of the steaming treatment is thought to be due to the higher mobility of metal

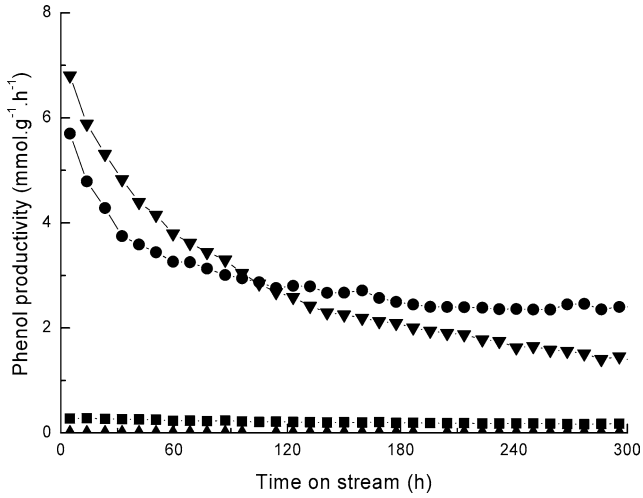

Fig. 2. Phenol productivity as a function of time-on-stream for steam-activated [Fe,Al]MFI (▼), steam-activated silicalite-1-Imp(Fe,Al) (●), steam-activated [Fe]MFI (■), and silicalite-1 (▲). Whereas the benzene selectivity for the [Fe,Al]MFI sample is 68% after 5 min and increases to over 98% only after 1 h, the benzene selectivity for steamed silicalite-1-Imp(Fe,Al) is close to 100% already directly at the start of the reaction.

oxide particles under hydrothermal conditions and their resulting redispersion to the micropore space, comparable to phenomena observed, for example, for molybdenum oxide [28,29]. We take these results as further support for our model of Fe–O–Al species as the active sites. One further observes that despite the somewhat lower initial activity the stability of the silicalite-1-derived zeolite is higher than that of [Fe,Al]MFI.

Finally, we note that the role of aluminum may not only be limited to generate Fe–O–Al species at extraframework positions that provide active centers for nitrous oxide decomposition and selective benzene oxidation but also to stabilize cationic Fe species as proposed by others [1,7,9,10,12,13,19–21]. In our view, these latter species can efficiently decompose nitrous oxide, thus explaining the much higher activity of over-exchanged systems in catalytic N_2O destruction compared to isomorphously substituted FeZSM-5 [14,15]. These catalysts generally show a low selectivity in benzene oxidation and only when the cationic Fe species have been removed by hydrothermal treatment a high selectively to phenol is obtained for these systems [15].

4. Conclusions

We have shown that there is a distinct difference in the reducibility of iron in Fe-silicalite and FeZSM-5 by following X-ray absorption spectra at the Fe *K* edge during temperature-programmed dehydration. Whereas a noticeable part of iron is reduced to ferrous ions in iron-containing aluminosilicalite, the ferric species in ferrosilicalite maintain their oxidation state. This explains the preference for aluminum-containing iron-zeolites to activate nitrous oxide,

an important step in the selective conversion of benzene to phenol with N_2O as oxidant. We propose that the large difference in reactivity of [Fe]MFI and [Fe,Al]MFI should not be ascribed to a higher active site density in [Fe,Al]MFI but to the chemical difference of iron in Fe–O–Al and Fe–O–Fe adducts. Active and more stable materials for benzene oxidation may be prepared by a simple dispersion of iron- and aluminum-oxide precursors in a silicalite-1 matrix.

References

[1] G. Centi, B. Wichterlova, A.T. Bell (Eds.), Catalysis by Unique Metal Ion Structures in Solid Matrices, in: NATO Science Series, Kluwer Academic, Dordrecht, 2001.
[2] G.I. Panov, CATTECH 4 (2000) 18.
[3] R. Burch, C. Howitt, Appl. Catal. A 103 (1993) 135.
[4] V.L. Zholobenko, I.N. Senchenya, L.M. Kustov, V.B. Kazansky, Kinet. Catal. 32 (1991) 151.
[5] L.M. Kustov, A.L. Tarasov, V.I. Bogdan, A.A. Tyrlov, J.W. Fulmer, Catal. Today 61 (2000) 123.
[6] J.L. Motz, H. Heinrichen, W.F. Hölderich, J. Mol. Catal. 136 (1998) 175.
[7] K.A. Dubkov, N.S. Ovanesyan, A.A. Shteinman, E.V. Starokon, G.I. Panov, J. Catal. 207 (2002) 341.
[8] E.J.M. Hensen, Q. Zhu, R.A. van Santen, J. Catal. 220 (2003) 260.
[9] V.I. Sobolev, G.I. Panov, A.S. Kharitonov, V.N. Romannikov, A.M. Volodin, K.G. Ione, J. Catal. 139 (1993) 435.
[10] G. Berlier, A. Zecchina, G. Spoto, G. Ricchiardi, S. Bordiga, C. Lamberti, J. Catal. 215 (2003) 264.
[11] D. Meloni, R. Monaci, V. Solinas, G. Berlier, S. Bordiga, I. Rossetti, C. Oliva, L. Forni, J. Catal. 214 (2003) 169.
[12] A.A. Battiston, J.H. Bitter, D.C. Koningsberger, Catal. Lett. 66 (2000) 75.
[13] P. Marturano, A. Kogelbauer, R. Prins, J. Catal. 190 (2000) 460.
[14] E.J.M. Hensen, Q. Zhu, M.M.R.M. Hendrix, A.R. Overweg, P.J. Kooyman, M. Sychev, R.A. van Santen, J. Catal. 221 (2004) 560.
[15] Q. Zhu, R.M. van Teeffelen, R.A. van Santen, E.J.M. Hensen, J. Catal. 221 (2004) 575.
[16] S. Bordiga, R. Buzzoni, F. Geobaldo, C. Lamberti, E. Giamello, A. Zecchina, G. Leofanti, G. Petrini, G. Tozzola, G. Vlaic, J. Catal. 158 (1996) 486.
[17] T.E. Westre, P. Kennepohl, J.G. DeWitt, B. Hedmann, K.O. Hodgson, E.I. Solomon, J. Am. Chem. Soc. 119 (1997) 6297.
[18] M. Wilke, F. Farges, P.-E. Petit, G.E. Brown Jr., F. Martin, Am. Miner. 86 (2001) 714.
[19] G. Berlier, G. Spoto, S. Bordiga, G. Ricchiardi, P. Fisicaro, A. Zecchina, I. Rossetti, E. Selli, L. Forni, E. Giamello, C. Lamberti, J. Catal. 208 (2002) 64.
[20] G. Berlier, G. Spoto, P. Fisicaro, S. Bordiga, A. Zecchina, E. Giamello, C. Lamberti, Microchem. J. 71 (2002) 101.
[21] J. Jia, Q. Sun, B. Wen, L.X. Chen, W.M.H. Sachtler, Catal. Lett. 82 (2002) 7.
[22] A.A. Battiston, J.H. Bitter, F.M.F. de Groot, A.R. Overweg, O. Stephan, J.A. van Bokhoven, P.J. Kooyman, C. van der Spek, G. Vankó, D.C. Koningsberger, J. Catal. 213 (2003) 251.
[23] A.A. Battiston, J.H. Bitter, W.M. Heijboer, F.M.F. de Groot, D.C. Koningsberger, J. Catal. 215 (2003) 279.
[24] A.A. Battiston, J.H. Bitter, D.C. Koningsberger, J. Catal. 218 (2003) 163.
[25] W.M. Heijboer, A.A. Battiston, A. Knop-Gericke, M. Hävecker, R. Mayer, H. Blum, R. Schlögl, B.M. Weckhuysen, D.C. Koningsberger, F.M.F. de Groot, J. Phys. Chem. B 107 (2003) 13069.
[26] S.H. Choi, B.R. Wood, J.A. Ryder, A.T. Bell, J. Phys. Chem. B 107 (2003) 11843.
[27] G. Pirngruber, J. Catal. 219 (2003) 456.
[28] A. Lopez Agudo, R. Cid, F. Orellana, J.L.G. Fierro, Polyhedron 5 (1986) 187.
[29] J.A. Anderson, B. Pawelec, J.L.G. Fierro, Appl. Catal. A: General 99 (1993) 37.